HEAVY QUARK PHYSICS AND THE CKM MATRIX*

M.S. Witherell

Department of Physics, University of California

Santa Barbara, CA 93106-9530, USA

Abstract

In this paper I discuss the Cabibbo-Kobayashi-Maskawa matrix, which is the source of CP violation in the Standard Model. I give the present experimental status, using the unitarity triangle to display the results and the predictions for the CP-violating asymmetries. Finally, I take increasingly speculative looks at 5 and 10 years into the future.

* Review given at the 1991 SLAC Summer Institute — Aug, 1991.

HEAVY QUARK PHYSICS AND THE CKM MATRIX

1. CP Violation, the CKM Matrix, and the Unitarity Triangle.

As is often pointed out, it is now 27 years after the initial discovery of CP violation, and we are still trying to understand its origin. It is encouraging that we have a natural explanation within the Standard Model: the Kobayashi-Maskawa hypothesis[1] that the CP-violating phase in the quark mixing (CKM) matrix is responsible for all CP violation. Yet we still have no experimental evidence confirming this hypothesis, and until we do CP violation will remain one of the most compelling issues in particle physics. As Fred Gilman posed the question,[2] we want to know whether (1) CP violation is a curiosity, perhaps a first glimpse at physics outside the scale of the Standard Model; or (2) it is a cornerstone of the Standard Model, completing the picture of the quark sector.

The CKM matrix elements can be defined using the amplitudes for W decay into $q\bar{q}$ final states: $M(W^+ \to Q\bar{q}) = M(W^+ \to e^+\nu_e)V_{Qq}$ where Q is a u-type quark and d-type quark. The matrix is then 3×3:

$$V_{Qq} = \begin{pmatrix} V_{ud} & V_{us} & V_{ub} \\ V_{cd} & V_{cs} & V_{cb} \\ V_{td} & V_{ts} & V_{tb} \end{pmatrix} \quad . \tag{1}$$

In the Standard Model, the matrix is unitary, and we now know that there are only three generations, at least of the familiar type. We know also that the off-diagonal elements are small, although the interesting physics we are now interested in depends critically on the size of these small elements. There are four independent parameters which define the matrix, three real rotation angles and one imaginary phase.

In the notation adopted by the Particle Data Group,[3] the matrix can be written

$$\begin{pmatrix} c_{12}c_{13} & s_{12}c_{13} & s_{13}\exp(-i\delta_{13}) \\ -s_{12}c_{23} & c_{12}c_{23} & c_{13}s_{23} \\ s_{12}s_{23} - c_{12}s_{13}c_{23}\exp(i\delta_{13}) & -c_{12}s_{23} & c_{13}c_{23} \end{pmatrix} \quad . \tag{2}$$

Here I keep only the leading terms for each element. This choice of parameterization conveniently isolates the CP-violating phase to the matrix elements which connect the first and third generations, V_{td} and V_{cb}. It is important to remember, however, that all CP amplitudes are proportional to the product of $s_{12}s_{13}s_{23}c_{12}c_{13}^2c_{23}\sin(\delta_{13})$. Thus all three mixing angles and the phase must be nonzero for CP to be violated.

Wolfenstein[4] made use of the fact that the off-diagonal elements are small to obtain a simple empirical representation:

$$\begin{pmatrix} 1-\lambda^2/2 & \lambda & A\lambda^3(\rho - i\eta) \\ -\lambda & 1-\lambda^2/2 & A\lambda^2 \\ A\lambda^3(1-\rho-i\eta) & -A\lambda^2 & 1 \end{pmatrix} \quad . \tag{3}$$

In fact, since $s_{12}/s_{23}/s_{13}$ are in the approximate ratio of $\lambda/\lambda^2/\lambda^3$, where λ is the Cabibbo angle, equal to 0.22, the parameters A and ρ are of order 1.

Unitarity imposes many conditions on these parameters, but the most interesting one is that $V_{ud}V_{ub}^* + V_{cd}V_{cb}^* + V_{td}V_{tb}^* = 0$. Making use of the fact that V_{ud} and V_{tb} are nearly unity, one gets $V_{ub}^* + V_{td} = |V_{cb}V_{cd}|$. This gives the triangle shown in Figure 1(a). If we divide all lengths in the triangle by the length of the base, we get the triangle shown in Fig. 1(b). The real and imaginary parts of the point A are just given by the parameters ρ and η which appear in V_{ub} and V_{td}.

The definitive test of the KM hypothesis is the observation of large, predictable asymmetries in B decays. The most direct connection between experiment and phenomenology comes in the decays of $B^0(\overline{B^0}) \to$ CP eigenstate. In

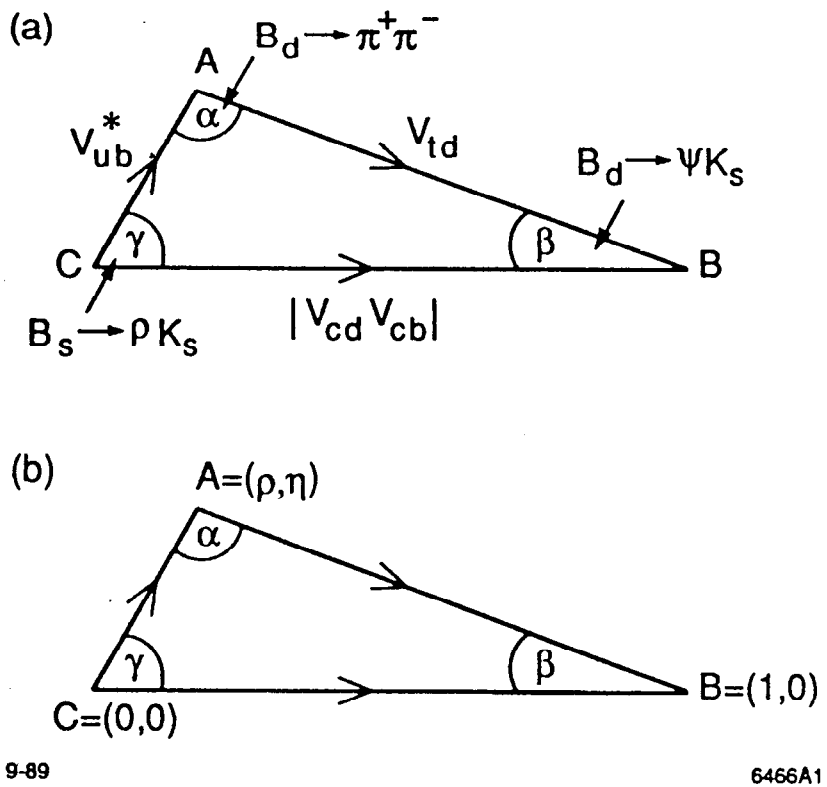

Figure 1. (a) Representation in the complex plane of the triangle formed by the CKM matrix elements using the relation $V_{ub}^* + V_{td} = |V_{cd}V_{cb}|$. (b) The rescaled triangle, with vertices at A(ρ,η), B(1,0), and C(0,0). Each angle is related to the CP-violation parameter for one class of B decay.

these modes the asymmetry is due to the interference of the direct decay path and one in which the B mixes before decaying. The usual time dependence of the decay rate is multiplied by a term $[1 \pm \sin(2\phi)\sin(x\Gamma t)]$, where ϕ is one of the three angles of the unitarity triangle. Thus there is an oscillation, of opposite sign for B^0 and $\overline{B^0}$, which has frequency $x\Gamma/2\pi$ and amplitude $\sin(2\phi)$. The measurement of the amplitude of this oscillation directly determines the angle ϕ, which is equal to β for decays such as $B_d \to \psi K_s$, α for $B_d \to \pi^+\pi^-$, and γ for $B_s \to \rho K_s$. Measuring CP violation with these asymmetries has two distinct advantages: the asymmetries are directly related to the CKM parameters, with minimal complication of hadronic matrix elements, and they are fairly large, for the present range of parameters.

2. Experimental Constraints on the CKM Matrix and the Unitarity Triangle

The measurements that determine the CKM matrix elements in the absence of unitarity constraints are shown in Table 1. When using unitarity, however, only V_{us}, V_{cb}, and V_{ub} are determined directly, since there are only 3 independent angles, ignoring the CP-violating phase. The numerical values of these three are (1) $|V_{ub}| = s_{12} = 0.2205 \pm 0.0018$, (2) $|V_{cb}| = s_{23} = 0.044 \pm 0.006$, and (3) $|V_{ub}/V_{cb}| = s_{13}/s_{23} = 0.11^{+0.07}_{-0.05}$. The errors for the last two are based on conservative estimates of theoretical uncertainties, as discussed below.

The shape of the unitary triangle is determined by the quantities ρ and η, as shown in Figure 1. One can completely specify the triangle using only CP-conserving measurements: V_{cd}, V_{cb}, $|V_{ub}|$, and $|V_{td}|$. Excluding the first of these, which is known very well, there are three amplitudes to determine experimentally. One gets an additional constraint from the ϵ parameter in K^0 decay,

	d	s	b
u	$n \to pe\nu$	$K \to \pi e\nu$ (*)	$b \to u\ell\nu$ (*)
c	$\nu d \to uc$	$D \to Ke\nu$	$B \to D^*\ell\nu$ (*)
t	$B_d \to \overline{B_d}$	$B_s \to \overline{B_s}$	

Table 1. Measurements which determine the CKM matrix. If 3-generation unitarity is used, however, only the three starred measurements are needed.

and the extraction of the amplitudes from the measured quantities depends on the top quark mass. Thus there are 5 experimental measurements relevant to specifying the triangle. Because of correlated errors, it is impossible to show the allowed region in one simple plot in ρ–η space.

Figure 2 shows the experimental constraints from present data, fixing the top quark mass to be 150 GeV, and assuming a value of $V_{cb} = 0.044$. The region between the two dotted circles is the region allowed by the measurement of V_{ub} from charmless B semileptonic decays. The two dashed circles correspond to the limits on the B_d mixing parameter, x_d. The two solid curves come from the measurement of ϵ in K_s decay. Since it is the only evidence of CP violation, ϵ is the only constraint that requires η to be nonzero. The shaded region shows the area allowed after all present experimental constraints are applied.

One can see immediately from Figure 2 the allowed range for the CP asymmetry parameters α and β defined in Fig. 1. For example, $\tan(\beta) = \eta/(1-\rho)$, which can range from 0.06 to 1.3. This corresponds to a range for the amplitude of the asymmetry, $\sin(2\beta)$ of 0.12 to 1.0. The value of $\sin(2\alpha)$ is completely unconstrained. I will now review briefly the five measurements which determine the allowed region, and discuss the experimental and theoretical uncertainties

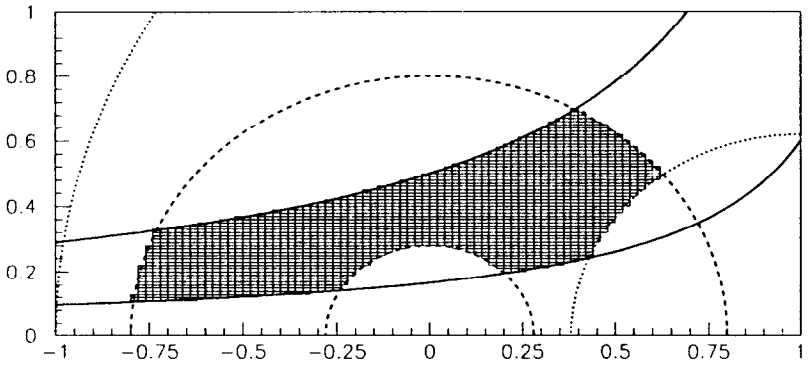

Figure 2. Constraints on the coordinates of point A of the rescaled unitarity triangle, for $m_t = 150$ GeV and $V_{cb} = 0.044$. The coordinates are ρ (horizontal) and η (vertical). The constraints come from measurements of $|V_{ub}/V_{cb}|$ (dashed circles), x_d (dotted circles), and ϵ (solid hyperbolas). The crosshatched region is allowed.

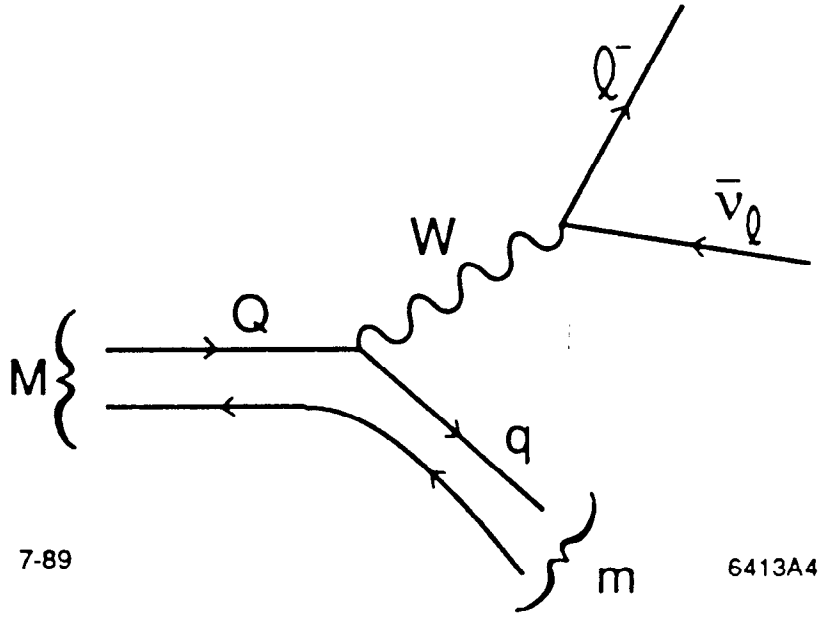

Figure 3. The diagram for semileptonic decay of a meson containing a heavy quark.

which limit our knowledge.

3. Measurements of V_{cb}

The CKM matrix elements V_{cb} and V_{ub} are measured in semileptonic decays of B mesons. We can separate the calculation of the amplitude for these decays into two parts (see Figure 3): a) the weak interaction, characterized by V_{cb} or V_{ub}, and b) the strong interaction — form factors which describe the amplitude for the final state quarks to recombine into specific mesons. The form factors depend on the momentum transfer variable $q^2 = M^2_{\ell\nu}$. For the pseudoscalar meson in the final state, such as D or π, there is only one important form factor, while for the vector mesons such as D* or ρ there are three. There is a very large literature, much of it very recent, on the calculation of these form factors, using valence quark models, quark sum rules, lattice gauge techniques, and heavy quark effective theory.

The CKM matrix element V_{cb} is measured in $b \to c$ semileptonic decays, using either the inclusive branching ratio, or the exclusive branching ratios $B \to D(D^*)\ell^+\nu$. The inclusive branching ratio is proportional to $m_b^5\ V_{cb}^2$. There is a large number of experimental measurements, listed in reference 3. One systematic uncertainty of all the experiments is due to the unknown fraction of $D^{**}\ell^+\nu$, which has a relatively soft lepton spectrum. The associated systematic error related to this has the same sign for all measurements, although with different magnitude. The approximate average value for the branching ratio is

$$B(B \to X\ell\nu) = 10.7 \pm 0.7\%.$$

There are additional systematic uncertainties in extracting V_{cb} from the inclusive branching ratio. For the simple free quark model, one has an uncertainty in the m_b^5 term. In the ACCMM inclusive model,[5] they deal with this by assuming a simple Fermi-momentum form for the quark and using the measured lepton spectrum to determine m_c/m_b and the mean Fermi momentum. The central value for V_{cb} using these various techniques with the inclusive branching ratio above is $0.047 \pm 0.002 \pm 0.005$. The last error represents the approximate uncertainty in the model assumptions.

The other approach in extracting V_{cb} is to use the measured branching ratios for the modes $B \to D(D^*)\ell\nu$. The signals in the D^* channel are especially clean, as shown in Fig. 4. The needed theoretical inputs are the exclusive form factors, which should be calculable, at least with some experimental help. Table 2 shows the measurements for these modes for CLEO and ARGUS, which agree well. The average branching ratios are $B(B \to D\ell\nu) = 1.6 \pm 0.4\%$ and $B(B \to D^*\ell\nu) = 4.4 \pm 0.7\%$. The value of V_{cb} from the D* measurement is $0.041 \pm 0.004 \pm 0.005$, where the last error is due to model dependence. Measuring the form factors directly from the data and comparing those with the models will help to reduce the model errors.

Mode	CLEO[6,7]	ARGUS[8]
$B^+ \to \overline{D^0}$	$1.6 \pm 0.6 \pm 0.2$	$1.5 \pm 0.5 \pm 0.3$
$B^0 \to D^-$	$1.8 \pm 0.6 \pm 0.3$	$1.5 \pm 0.5 \pm 0.3$
$B^+ \to \overline{D^{*0}}$	$4.1 \pm 0.8 \pm 0.8$	$4.4 \pm 0.6 \pm 0.5$
$B^0 \to D^{*-}$	$4.6 \pm 0.5 \pm 0.7$	$4.4 \pm 0.6 \pm 0.5$

Table 2. Measurements of exclusive b → c semileptonic branching ratios, in percent.

An alternative way of interpreting the exclusive measurements has been put

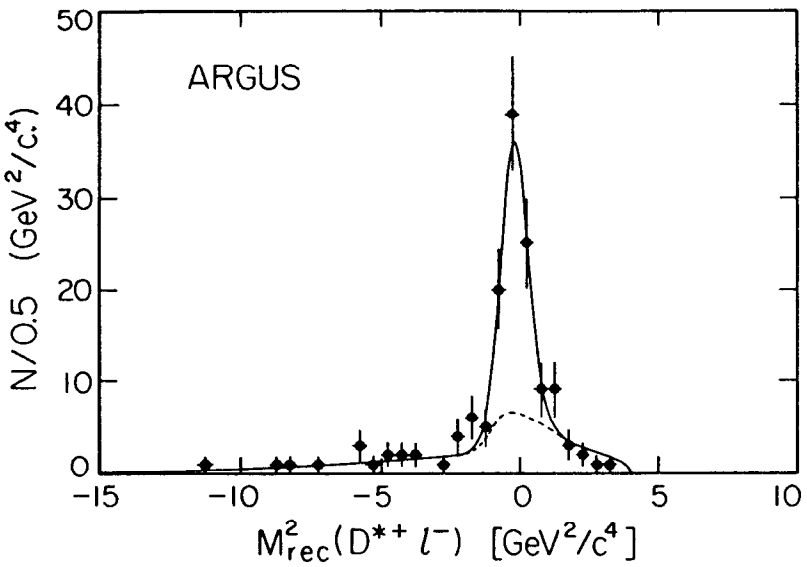

Figure 4. The plot of mass^2 recoiling against the D^{*+} + lepton in ARGUS data. The $B \to D^{*+}\ell^-\nu$ decays appear as a large peak with zero recoil mass. CLEO has similar data.

forward by Neubert.[9] This uses the fact that in the heavy quark limit, the form factors are calculable at $q^2 = q^2_{max}$, which corresponds to the case of the D(D*) meson at rest. The fundamental principle is that the wave function of a meson consisting of a heavy quark and a light antiquark does not depend on the properties of the heavy quark. There are corrections to the heavy quark limit of order $1/M_c$ and α_s, which are calculated. The q^2 dependence of the form factors comes from a universal function, the Wise-Isgur function.[10]

In Neubert's approach, the Wise-Isgur function is evaluated using the data. The $D^*\ell\nu$ decay is used because the corrections to the heavy quark limit are small, and because the decay rate is larger near the kinematic limit at q^2_{max}. The resulting value of $V_{cb} = 0.045 \pm 0.007$. Taking into account all of these methods, I will take as the best value $\underline{V_{cb} = 0.044 \pm 0.006}$.

4. Measurements of V_{ub}

ARGUS and CLEO have reported excess leptons at the $\Upsilon(4s)$ with $p = 2.3 - 2.6$ GeV/c, which represents the first evidence of $b \to u$ transitions. Figure 5 shows the experimental evidence. The quantitative interpretation of this result to obtain V_{ub}/V_{cb} is much more difficult than for the case of V_{cb}, however. In principle, the inclusive decay $b \to u\ell\nu$ is a case in which the free quark model should work well, because the energy release in the decay is so large compared to the final state quark mass. The signal is only seen at the endpoint region, however, where a few final states (π, ρ, ω) dominate. It is exactly in this resonance region that the free quark model is least reliable.

The exclusive models are also not adequate, however. The quark models are suspect because of the light final state quark. In fact, we know that in the one similar case we can check, the measured value of $\Gamma(D \to K^*e\nu)$ is about 0.6 of

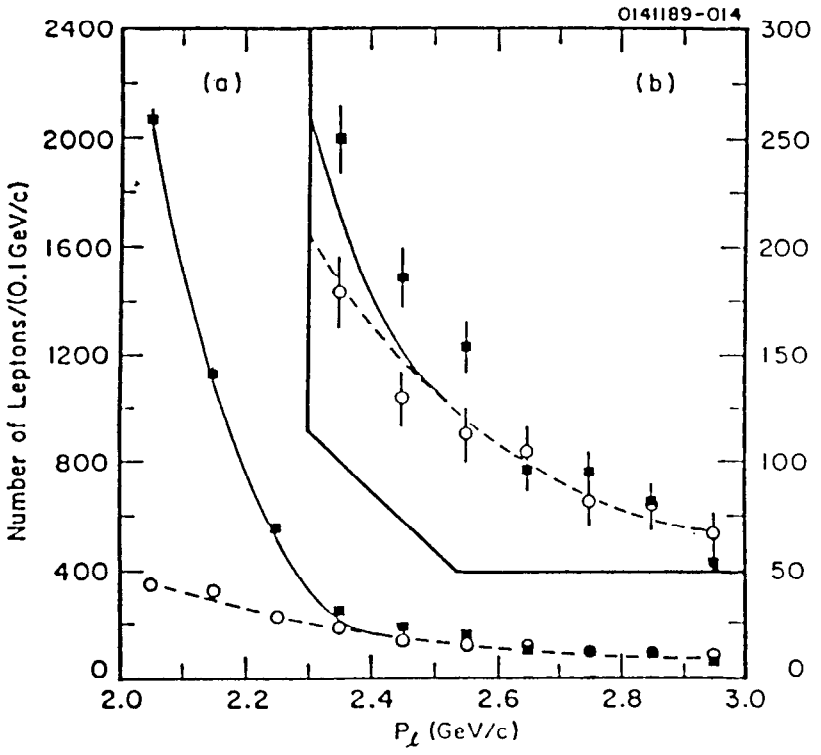

Figure 5. The lepton spectrum near the b → c endpoint region in CLEO data. The solid squares represent Υ(4s) data, the circles scaled continuum data. The curve gives the expected spectrum if $V_{ub} = 0$. The excess in the region 2.3–2.6 GeV is due to b → u transitions. ARGUS has similar data.

that predicted. There is a completely separate problem in the case of B decay, however, due to the unknown q^2 dependence of the form factor. The form factor squared varies by a factor of 100 over the Dalitz plot, and we have no reliable way of calculating the q^2 dependence. Figure 6 shows the Dalitz plot boundaries for $B \to \pi(\rho)\ell\nu$. The B^* pole is only just beyond the $\pi\ell\nu$ kinematic limit, which is why the q^2 dependence is likely to be very strong.

Table 3 shows the results on V_{ub}/V_{cb} for the two experiments, using six different models. Obviously, the model error already dominates, even though the experimental error is large. In fact, we expect that the spread among the models is an underestimate of the error, for a couple of reasons. The discrepancy with experiment in charm semileptonic decay is greater than the differences between models, suggesting a similar problem in the very similar $b \to u$ decay. In addition, all of the models use a more or less common q^2 dependence for the form factors.

Model	CLEO[11]	ARGUS[12]
ACM[5]	.09 ± .01	.11 ± .01
ISGW[13]	.15 ± .02	.20 ± .02
WBS[14]	.11 ± .01	.13 ± .02
KS[15]	.10 ± .01	.11 ± .01
RDB[16]	.12 ± .02	
KP[17]		.15 ± .02

Table 3. Determinations of V_{ub}/V_{cb} using different models.

Although this is not an exact procedure, I will take as a best value $V_{ub}/V_{cb} = 0.11^{+0.07}_{-0.05}$. There is a recent report from ARGUS of an exclusive decay mode,[18] $B^+ \to \rho^0\ell\nu$, which corresponds to a value of $0.15^{+0.15}_{-0.05}$, which is less accurate

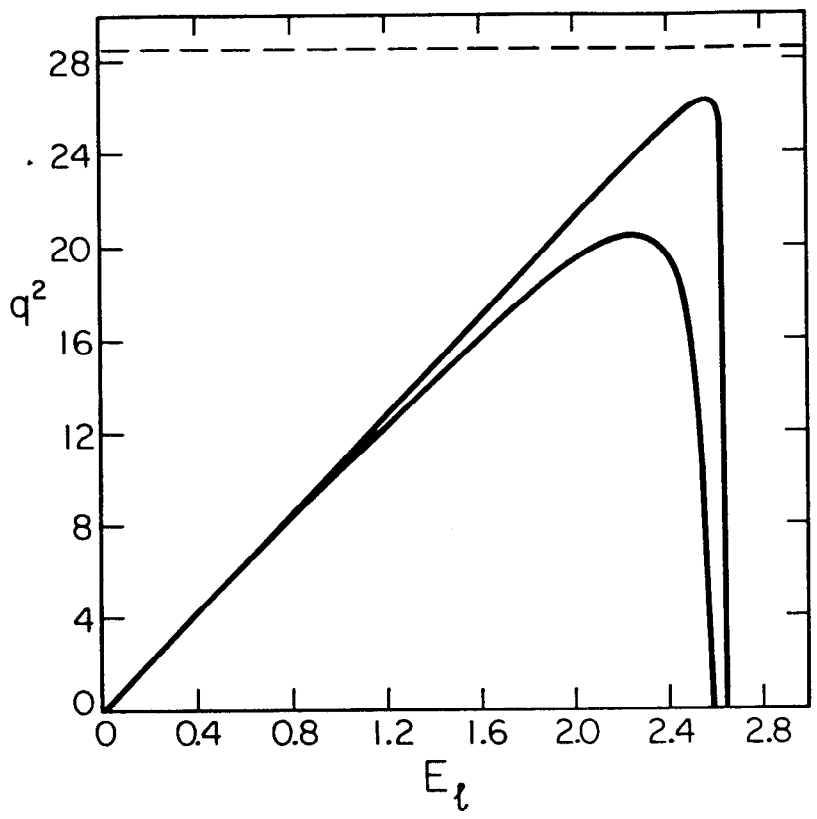

Figure 6. The Dalitz plot for b $\rightarrow$ u$\ell\nu$ decays. The coordinates are lepton energy and $q^2 = M^2(\ell\nu)$. The upper curve corresponds to B $\rightarrow \pi\ell\nu$, the lower B $\rightarrow \rho\ell\nu$. The dashed horizontal line gives the position of the B* pole expected in the form factor.

than but in agreement with the first measurements.

To improve our knowledge of this crucial CKM parameter will require progress on a broad front. We need better charm form factor measurements, to serve as a check of the form factor models, and measurements of the exclusive decays $B \rightarrow (\rho, \omega, \pi)\ell\nu$ over the full q^2 range. It is essential to check the rates over the Dalitz plot, and it will be impossible to separate $b \rightarrow u$ inclusive decays below the $b \rightarrow c$ endpoint energy. Finally we will need theoretical advances, making use of the experimental data, to reduce the uncertainty in form factors.

5. B_d Mixing, the B Decay Constant, and B_s Mixing

The principal diagram for b_d mixing is shown in Figure 7. With the very heavy top quark mass which we now know exists, the top quark loop dominates. The measured parameter

$$x_d = \Delta M/\Gamma \propto V_{tb}^2\, V_{td}^2\, f_B^2\, B_B\, m_t^2\, F(m_t/m_W)^2. \qquad (4)$$

The last function F is approximately proportional to $m_t^{-0.4}$ in the region of interest.[18] Thus V_{td} varies inversely with the theoretic al value of $f_B B_B^{1/2}$, which is very poorly known—0.1–0.3 GeV. There are smaller but significant errors on V_{td} due to the measurement errors on x_d and the unknown value of the top quark mass.

The present experimental measurement[20] of $x_d = 0.67 \pm 0.15$ corresponds to a value of $V_{td} = (0.010 - 0.033)(m_t/m_W)^{-0.8}$. Thus one gets limits which are circles centered at $\rho = 1$, $\eta = 0$. The present uncertainty is so large that it barely cuts into the allowed region in Figure 2.

The dominant uncertainty in the CP-violating parameter sin(2β) is due to

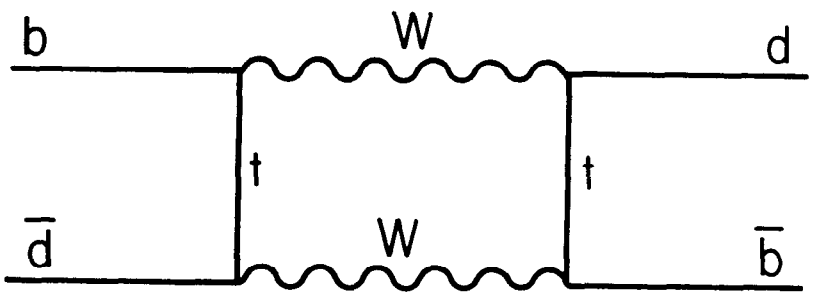

Figure 7. The diagram for $B\bar{B}$ mixing.

the large error on V_{td}, which in turn is due to the error on the B decay constant f_B. Schmidtler and Schubert[20] compiled ten recent theoretical estimates of the B meson decay constant. Most of the results are in the range 100–200 MeV, with the major exception of the lattice gauge calculation of the Rome-Southampton group.[21] Their results disagree with the usual scaling law that $f_B = f_D(M_D/M_B)^{1/2}$, and they find $f_B \simeq 300$ MeV.

In that paper, Schmidtler and Schubert (and Kim, Rosner, and Yuan[22] in a similar paper) investigate what happens to the allowed region as f_B goes from 100 to 300 MeV. They calculate a maximum likelihood in the two-dimensional ρ–η space, under the assumption of no error in f_B and no model uncertainty in measuring V_{ub}. They then allow f_B to vary, and find that the preferred values of (ρ, η) lie around (-0.4,+0.2) for low f_B, but at around 175 MeV there is a transition to values near (+0.3,+0.3). This transition from the second to the first quadrant changes the CP violation asymmetry $\sin(2\beta)$ from about 0.3 to about 0.8, which dramatically alters the prospect for observing the effect.

One way of experimentally measuring V_{td} without needing to know f_B accurately is to measure B_s mixing. It is straightforward to see from Figure 7 that the two mixing parameters are related:

$$\frac{xd}{xs} = \frac{|V_{td}|^2 f_d^2}{|V_{ts}|^2 f_s^2} \simeq \frac{|V_{td}|^2}{|V_{ts}|^2}. \tag{5}$$

The expected value of x_s depends on f_B^2, and the present allowed range is from 4 to 50. The two possibilities of Schmidtler and Schubert correspond to (a) $f_B = 150$ MeV, $x_s = 8$ and $\sin(2\beta) = 0.3$, and (b) $f_B = 250$ MeV, $x_s = 30$ and $\sin(2\beta) = 0.8$. In the first case x_s is measurable, although with some difficulty; in the second, f_B is too large to be measured in the foreseeable future, but the CP violating asymmetry is relatively easy to observe.

6. CP Violation in the K^0 System

The only CP violation seen to date is in the K^0 system, and the only CP parameter which is unambiguously nonzero is ϵ. The parameter ϵ is the imaginary part of the amplitude for a mixing diagram that is similar to Figure 7, but in which both both c quarks and t quarks are important in the loop. The value of ϵ calculated this way is

$$\epsilon \propto B_K \, V_{cb}^2 \eta [1 + 1.3(V_{cb}/0.044)^2 \, (1-\rho) \, (m_t/m_W)^{1.6}]. \qquad (6)$$

The first term in the bracket represents one c and one t quark in the loop, the second term two t quarks.

The measurement of $|\epsilon|$ of 2.27×10^{-3} has very little uncertainty. There are large uncertainties in B_K, m_t, and V_{cb}, however. In particular, there is a factor of 3 uncertainty in B_K, which causes a factor of 3 uncertainty in determining η.

The other experimental constraint comes from the measurements of ϵ'/ϵ. At fixed m_t, $\epsilon'/\epsilon \propto |V_{cb}|^2 \eta f(m_t)$. According to recent work,[22] the function $f(m_t)$ changes by about an order of magnitude over the allowed range of m_t. Thus there is no additional constraint on η using present knowledge. Unfortunately, the theoretical uncertainty on η is about 50% from uncertainties in m_s and $\Lambda_{\rm QCD}$, even if m_t is known. Thus, although it is crucial to measure ϵ'/ϵ as accurately as possible to test consistency with the theory, it is much more difficult to use the measurement to constrain the value of CKM parameters.

7. Effects of the Top Quark Mass and V_{cb}

The lack of knowledge of the top quark mass has two important effects, which are suppressed in Figure 2. The allowed circles for V_{td} from B_d mixing shrink in radius like $(m_t)^{-0.8}$. This is apparent from Eq. 4. Secondly, the values of η on the limiting hyperbolas derived from ϵ are reduced like $(m_t)^{-1.6}$, approximately. This is because the second term in equation 6 is dominant for the top quark masses of interest.

Figure 8 shows the allowed region, analogous to that of Figure 2, for a top quark mass of 100 and 200 GeV. The changes are rather dramatic, but the allowed region for the CKM parameters is large enough that there is no useful constraint on m_t. To first approximation, the allowed region moves toward the lower right-hand corner of the plot with higher top quark mass.

One gets a similar migration of the allowed region with V_{cb}. The limit circles in Figure 2 from V_{ub}/V_{cb} do not move, but the circles due to x_d mixing Figure 9 shows the allowed region for V_{cb} values of 0.037 and 0.051. Surprisingly, even within the apparently small range of V_{cb} allowed by present experiments there are significant changes in the shape of the unitarity triangle.

8. The Status of CKM — 1996

Having reviewed what new information is needed to improve our knowledge of the CKM matrix, it is tempting to look forward at what the status might be in five years. This is clearly a dangerous procedure, since we know that five-year plans for progress in research do not work very well. Nonetheless, it is time for some comic relief. Let us imagine a review talk in 1996.

After a fierce competition, both CDF and D0 have announced observation of the top quark in data from the 1992–93, at a Fermilab press conference. There are no anomalies in the events, and the mass is measured to be 140 ± 15 GeV.

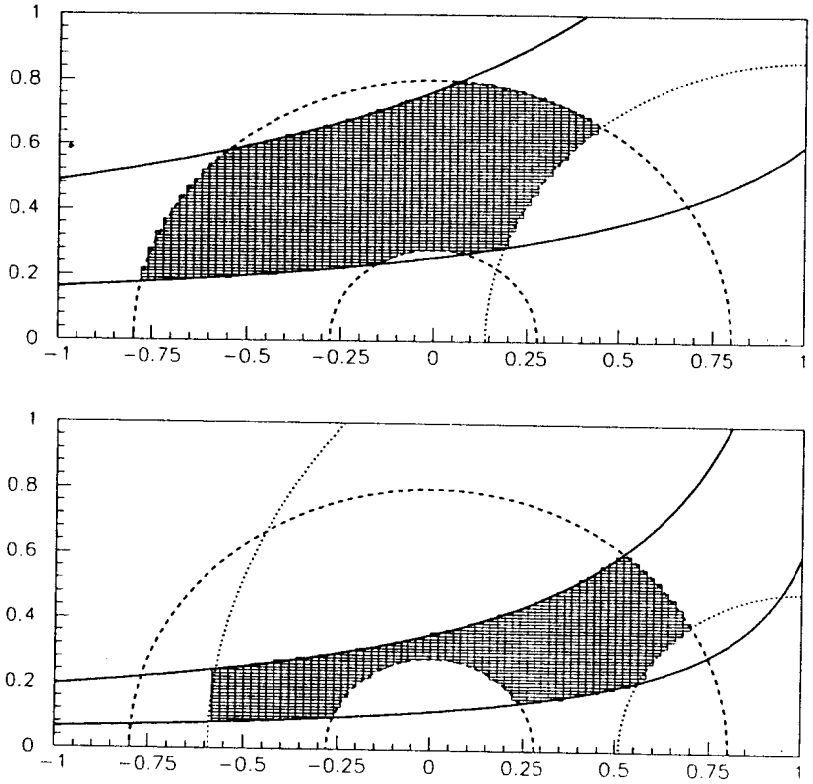

Figure 8. Constraints on the rescaled unitarity triangle, similar to Figure 2, for (a) $m_t = 100$ GeV, (b) $m_t = 200$ GeV.

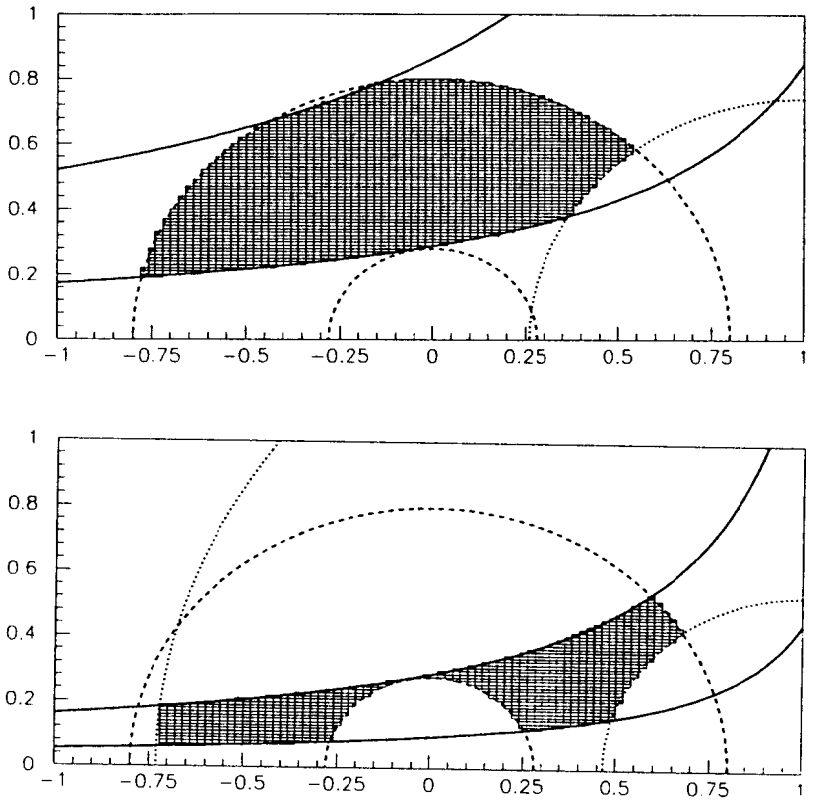

Figure 9. Constraints on the rescaled unitarity triangle, similar to Figure 2, for (a) $V_{cb} = 0.037$ and $V_{cb} = 0.051$.

CLEO and ARGUS have measured the $B \to D^* \ell \nu$ and have completed the full form factor analysis. The value of V_{cb} is now 0.044 ± 0.002. E687, E791, CLEO, and ARGUS have improved the measurement of the charm form factors, and refined form factor models and lattice gauge calculations agree with the data and each other. Most recently, the decay modes $B \to \rho \ell \nu$ and $\omega \ell \nu$ have been measured, with some form factor information. As a result of all this work, the best value of $V_{ub}/V_{cb} = 0.12 \pm 0.03$.

The mixing parameter x_d has been measured somewhat better. More importantly, the range of f_B has been narrowed to the range 130–180 GeV, removing the ambiguity discussed in section 5. As a result, the circles corresponding to limits on $[(1-\rho)^2 + \eta^2]^{1/2}$ are now bounded at 1.25 and 2.0.

Figure 10 shows the allowed region using all of the information available in this version of 1996. The allowed area has been reduced by a factor of about 4. The improvement is even larger than this, however, since the variations due to top quark mass and V_{cb} have been almost completely removed. The CP asymmetries are somewhat more restricted, but still range fairly widely.

9. 2001

Practicing futurism is addictive. Talking about the results expected in five years soon leads to discussing the future 10 years hence. We are now in a different regime, however, since the progress depends on machines not yet built, and more importantly not yet funded. I will go ahead and picture what things might look like with some optimism about what facilities are available. Perhaps the predictions will be right, but with the year wrong. I will also be purposely vague about which experiment provides the best information. In fact, I am even vague about where some machines are located!

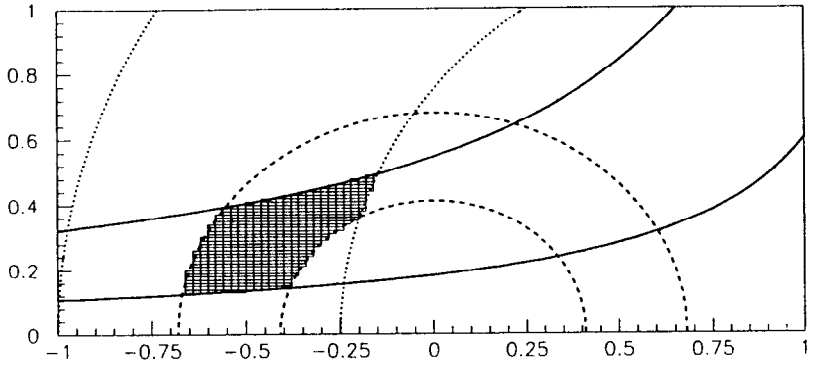

Figure 10. Future constraints on the rescaled unitarity triangle, under the speculative assumptions listed for the status in 1996.

We imagine that by 2001 B_s mixing has been observed, by some combination of hadron colliders and LEP. The value of x_s is 7 ± 2, which corresponds to a fast oscillation, but not too fast to observe. V_{cb} has been measured somewhat better, but more important is the dramatic improvement in V_{ub}. Using tagged B's at the B factory, it has been possible to extract clean signals over the entire Dalitz plot, and detailed form factor information. The value of V_{ub}/V_{cb} is 0.12 ± 0.01. Finally, the K_s experiments at FNAL and CERN have measured ϵ'/ϵ quite precisely, giving a value of $(3.5 \pm 1.0) \times 10^{-4}$. With the known top quark mass, and the fairly large uncertainty in the matrix element, the value of η extracted from this result is 0.30 ± 0.12.

Figure 11 shows the allowed region in ρ–η space with all of these measurements. The allowed area has been decreased by another large factor. In addition, there is an important consistency check provided by the measurement of ϵ'. One has very well defined predictions for both of the CP violating angles, α and β.

We speculate that by 2001 CP violation has been measured in a number of modes. Using the Main Injector, CDF and D0 have seen the asymmetries in the mode $B \to \psi K_s$, and measured $\sin(2\beta)$ with an error of ± 0.16. At the B factory, $\sin(2\beta)$ is measured with a precision of ± 0.06, and $\sin(2\alpha)$ is measured almost as well using the modes $\pi\pi$ and $\rho\pi$. The results are $\sin(2\beta) = 0.32 \pm 0.06$ and $\sin(2\alpha) = 0.56 \pm 0.08$. Figure 12 shows the constraints from these two measurements.

As we said at the beginning of this paper, the characteristic signature of the KM hypothesis is large and predictable asymmetries in B decays, in particular to CP eigenstates. Looking at Figures 11 and 12, it is obvious that a definitive and detailed test of these predictions is within reach. If CP violation is from

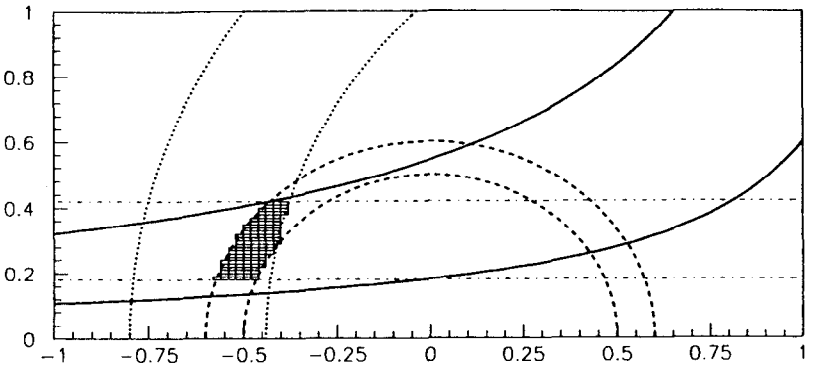

Figure 11. Future constraints on the rescaled unitarity triangle, under the even more speculative assumptions listed for the status in 2001. The horizontal dot-dashed lines represent the constraints from measurements of ϵ'/ϵ.

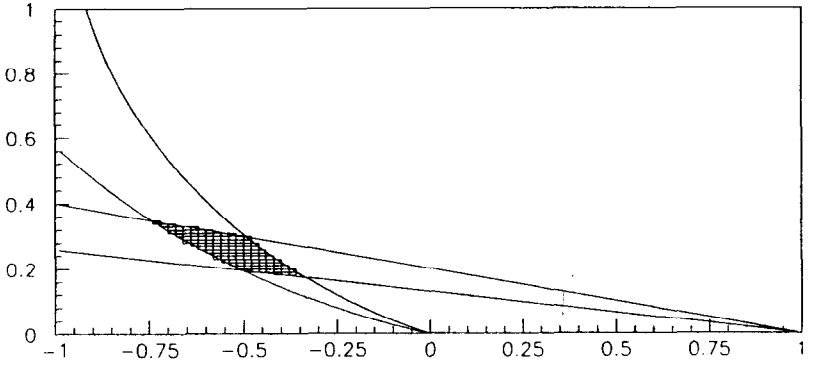

Figure 12. Constraints on the rescaled unitarity triangle that would result from future measurements of CP violating asymmetries with the precision quoted in the text.

some other source, or is not solely due to the CKM phase, the asymmetries can be totally unrelated to the predictions we have discussed.[23] This would be the most dramatic outcome to this series of measurements.

10. Conclusions

I now return to the realities of 1991. It is clear that one of the most fundamental tests of the standard model is the verification of the KM hypothesis for CP violation, which is now a cornerstone of that model. The experimental manifestation of this hypothesis is the observation of large, predictable asymmetries in the decays of B mesons, especially in those to CP eigenstates.

The expected asymmetries are demonstrated most clearly through the unitarity triangle. The present experiments determine the shape of this triangle rather poorly. An ambitious program of experimental measurement and theoretical work will steadily improve the picture over the next few years.

Experiments are planned which will obtain precise measurements of the CP asymmetries in many modes. These will provide the first check of whether we understand anything about the source of CP violation. In addition, we will be able to make sensitive checks of whether the K-M picture is the complete story of CP violation. Since this program involves a close look at corners of the Standard Model which are unexplored, it provides one of the best hopes of finding unexpected new physics. The chief obstacle to progress is that all of the experiments which will provide definitive answers to these questions require new accelerator facilities.

Acknowledgments

I have drawn from many of the treatments of this material, besides the listed references. I have benefited from papers on semileptonic decay by Gilman and Singleton, and Stone. Discussions of the CKM matrix and unitarity triangles by Dib, Dunietz, Nir, and Gilman and by Bjorken were very helpful. Projections of future measurements are based primarily on the SLAC and Cornell B-factory documents, and upgrade proposals for CDF and D0.

References

1. M. Kobayashi and R. Maskawa, *Prog. Theor. Phys.* **49**, 652 (1973).
2. F.J. Gilman in "Physics at the 100 GeV Mass Scale", the Proceedings of the 17th SLAC Summer Institute on Particle Physics, SLAC-Report-361 (1989).
3. Particle Data Group, *Phys. Lett.* **B239**, 1 (1990).
4. L. Wolfenstein, *Phys. Rev. Lett.* , 51 (1945), 1983.
5. G. Altarelli *et al.*, *Nucl. Phys.* **B208**, 365 (1982).
6. R. Fulton *et al.*, *Phys. Rev. D* **43**, 651 (1991).
7. D. Bortoletto *et al.*, *Phys. Rev. Lett.* **63**, 1667 (1989).
8. H. Albrecht *et al.*, *Phys. Lett.* **B219**, 121 (1989), and *Phys. Lett.* **B229**, 175 (1990); as slightly revised by M. Danilov, in paper at 1991 Lepton-Photon Conference.
9. M. Neubert, Heidelberg preprint HD-THEP 91-13.
10. N. Isgur and M.B. Wise, *Phys. Lett.* **B232**, 113 (1989) and **B237**, 527 (1990).
11. R. Fulton *et al.*, *Phys. Rev. Lett.* **64**, 16 (1990).
12. H. Albrecht *et al.*, *Phys. Lett.* **B255**, 297 (1991).
13. N. Isgur, D. Scora, B. Grinstein, and M.B. Wise, *Phys. Rev. D* **39**, 799 (1989).
14. M. Wirbel, B. Stech, and M. Bauer, *Z. Phys.* **C38**, 511 (1988).
15. J.G. Koerner and G.A. Schuler, *Z. Phys.* **C38**, 591 (1988).
16. C. Ramirez, J.F. Donoghue, and G. Burdman, *Phys. Rev. D* **41**, 1496 (1990).
17. G. Kramer and W.F. Palmer, *Phys. Rev. D* **42**, 85 (1990).
18. D. Britton, these proceedings.
19. L. Wolfenstein, paper presented at the International Symposium on Heavy Flavors, Orsay, June 1991.

20. M. Schmidtler and K.R. Schubert, Karlsruhe report IEKP-KA/91-4 gives this value of x_d as an average based on M. Artuso *et al.*, *Phys. Rev. Lett.* **62**, 2233 (1989); and H. Albrecht *et al.*, *Phys. Lett.* **B192**, 245 (1987).

21. C.R. Allton *et al.*, *Nucl. Phys.* **B349**, 598 (1991).

22. C.S. Kim, J.L. Rosner, and C.-P. Yuan, Chicago preprint EFI 89-47.

23. G. Buchalla, A.J. Buras, and M.K. Harlander, *Nucl. Phys.* **B349**, 1 (1991).

24. Y. Nir and D.J. Silverman, *Nucl. Phys.* **B345**, 301 (1991).